

# Wake developments behind different configurations of passive disks and active rotors

V L Okulov<sup>1,2</sup>, I V Litvinov<sup>2</sup>, R F Mikkelsen<sup>1</sup>, I V Naumov<sup>2</sup>, J N Sørensen<sup>1</sup>

<sup>1</sup>Department of Wind Energy, Technical University of Denmark, Lyngby, Denmark

<sup>2</sup>Kutateladze Institute of Thermophysics SB RAS, Novosibirsk, Russia

E-mail: vaok@dtu.dk

**Abstract.** The present paper takes a broad view on our previous experimental studies of flows behind different single and dual configurations from passive disks or active rotors to establish new aspects of the wake development [1-4]. The aim of the present examination is to obtain a better understanding of the wake formations and interactions between wind turbines in wind farms. A correlation between independent investigations of the near [1] and far wakes behind single [2] and dual [3-4] systems will be established to the same operating regimes and flow conditions. New examinations of the old data need because two main differences in the wake behaviour for the disk-disk and the rotor-rotor systems were found: the wake intensity grows for the dual disks in comparison with the single one, but in contrast to this, wake intensity behind the dual rotor system is smaller than the one behind a single rotor. These differences may be explained by an influence of the rotor tip vortices which are absent in the disk-disk model. The present retesting of the near and far wake data should provide an evidence of this conclusion.

## 1. Introduction

In spite of the extensive investigations of turbine interaction in wind farms, the prediction of the available power and structural stability of wind turbines located in the wake of other turbines in a wind farm are still open questions [5-6].

In the present paper, we will compare the wakes behind solitary setups containing a solid disk (D) or a three-bladed HAWT rotor (R); dual coaxial models consisting of either two identical rotors (R-R) or two identical disks (D-D), and a mixing coaxial model including both single disk and rotor (D-R). In the comparison, we used the solid disk because both disk and rotor far wakes have inherited similar Strouhal oscillations [1]. All systems were studied at the same spatial positions in a uniform inflow of the water flume [1-4] and the dual systems were investigated for different interspatial distances along the setup axis,  $L_x = 4, 6$  and  $8D$ . The investigations were carried out in the water flume of length 35m, 3m width and an operative height of 0.9m. The 3m wide test section is fitted with transparent walls at a distance of 20 m from the channel inlet. The freestream flow speed in the flume was  $U_0 = 0.54$  m/s. The axis of setup with the rotors or disks was positioned at a height of 0.5m from the channel bottom and 1.5 m away from the two walls of the flume. The experimental setup is basically the same as in [1-4] with the disk diameter  $D_d = 0.3$  m and the three-bladed rotors have a blade length of 0.159 m.

The purpose of the analysis is to reconstruct and compare the wake developments and decays behind all systems to recognize and describe factors impacting on the wake formation and evolution. The present retesting of both near and far wake data should provide an evidence of a significant role of the tip vortices in the rotor which are absent and could not effect on the wakes behind the disks.



## 2. Dissimilar behavior of far wakes behind different dual systems

New examinations of the old data need because two main differences in the far wake behavior for the D-D and R-R systems were found in [3]. The wake intensity grows for the dual disks in comparison with the single one, but in contrast to this, wake intensity behind the dual rotor system is smaller than the one behind a single rotor. Fig. 1 shows downstream variations of the maximum axial velocity deficit  $\frac{\Delta U}{U_0} = \frac{U_0 - U}{U_0}$  in the wake behind all possible configurations ( $U$  is velocity on the setup axis): the single D and R [2]; the D-D [3], D-R [4] and the R-R [3] setups for the different distances of the dual systems:  $L_x = 4, 6, 8D$ .

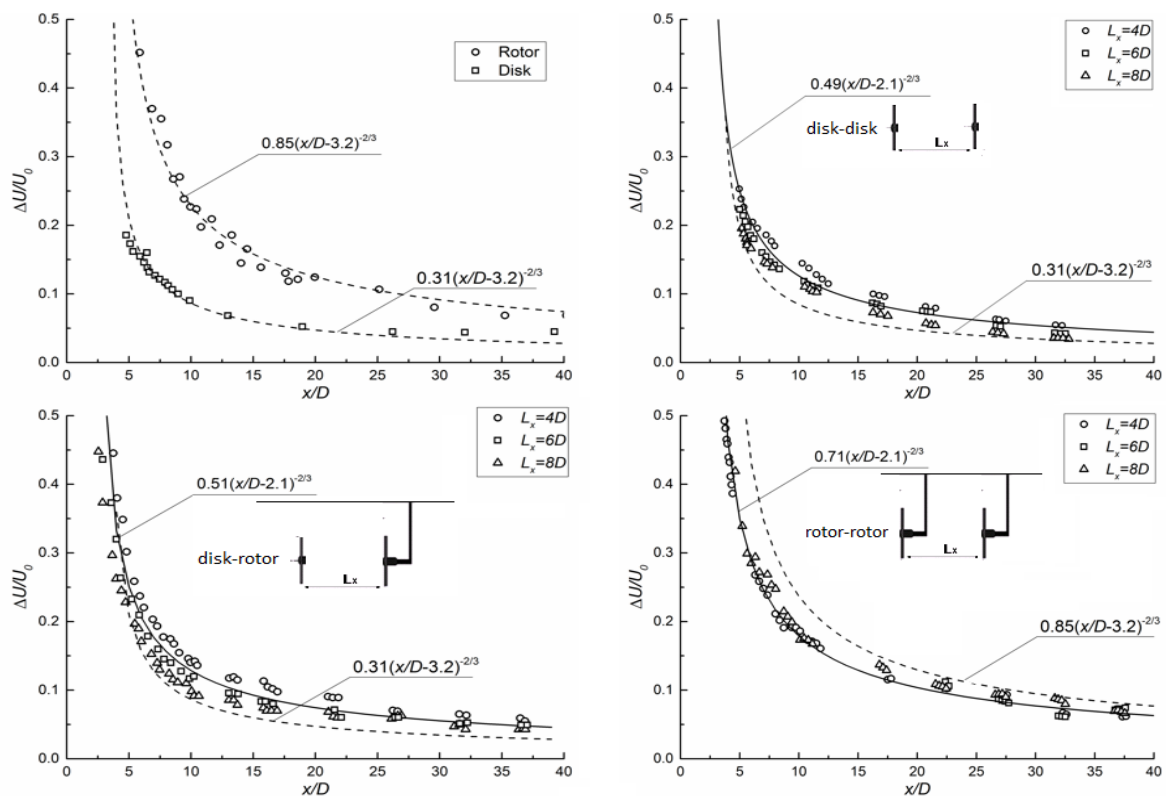


**Figure 1.** Far wakes of the different dual configurations. Dashed lines indicate both single cases.

The experimental data using regression techniques to fit all velocity profiles were approximated by a rational function  $G(x) = \Delta U(x)/U_0 = a(x - x_0)^{-2/3}$  (lines on Fig. 1), where the attenuation constants  $a$  and  $x_0$  are collected in table 1.

**Table 1.** The attenuation constants for the single and dual configurations of the disk or rotor setups.

Type of the setup	$a$	$x_0$
Single disk	0.31	3.2
D-D	0.49	2.1
D-R (optimal R)	0.51	2.1
R-R (optimal R and R)	0.71	2.1
Single rotor (optimal R)	0.85	3.2

As seen from all graphs of Fig. 1, the velocity deficits of the far wakes from all single and dual configurations are well described by this rational function with the same exponent  $(-2/3)$  and the different values of the attenuation constants (Table 1). For clarity, the first graph shows the wake developments only for the single disk [8] or rotor [9]. The disk just as a passive flow damper and the rotor as an active energy conversion explain the difference in the strengths of both wakes.

For all dual systems in which the disk placed at a forward position, the data on the next two plots of Fig. 1 and the corresponding constants of Table 1 indicate some growth of the velocity deficits in the far wakes as compared with ones behind the single disk. Fig. 1 also shows that the total wake deficit increases in the both cases (D-D and D-R) when the distance between the first disk and second element decreases from  $L_x = 8D$  to  $4D$ . A damping influence of the second disk or rotor on the initial wake behind the forward passive disk produces the extra velocity deficit for both cases (D-D and D-R) too.

The last plot of Fig. 1 shows the wake behavior behind two active wind turbine rotors (R-R) extracting power from the flow at the optimal operating conditions of both ones.

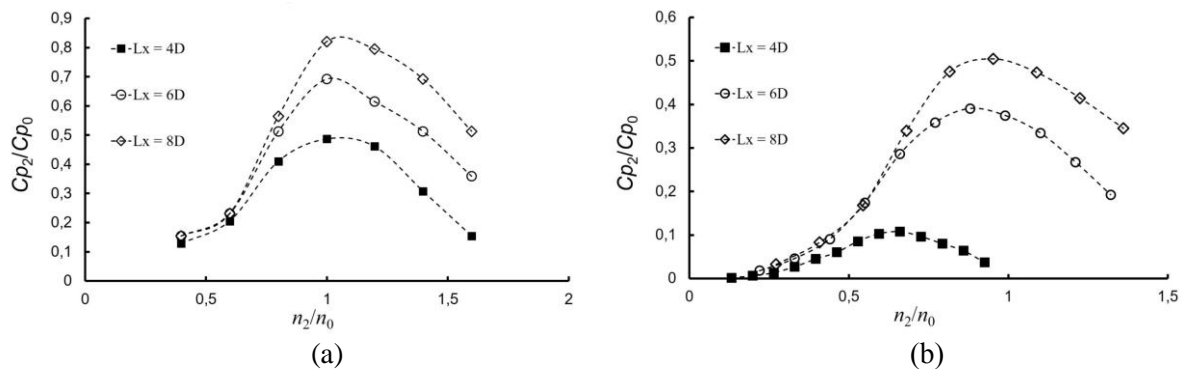


**Figure 2.** Variations of the power coefficients of the second rotors in the setups: (a) D-R and (b) R-R.

For the first rotor an angular velocity of the servo drive,  $n_1 \equiv n_0 = 2.29$  rps, coincides to the design TSR of the single rotor ( $\lambda_1 \equiv \lambda_0 = 5$ ) with the maximal power coefficient  $C_{p0} = 0.37$  and the incoming freestream flow ( $U_1 \equiv U_0 = 0.54$  m/s). An evolution of the optimal operating regimes for the second rotor in both D-R and R-R cases is not such a simple task since the velocity  $U_2$  of the incident flow upstream from the second rotor is not known and not uniform behind either the forward disk or rotor. The optimal angular velocity of the servo drive ( $n_2$ ) in the both cases were varied until optimum power conditions ( $\max C_{p2}$ ) were achieved (Fig.2 and Table 2) [4, 10].

**Table 2.** Operating parameters of the dual setups.

Types of the setup	Parameters	Values		
	$L_x$ - distance	4D	6D	8D
D-D	$U_2/U_0$	0.41	0.58	0.61
	$(C_{T2} + C_{T1})/C_{T0}$	1.69	1.86	1.97
	$\max C_{p2}/C_{p0}$	0.48	0.69	0.83
D-R (optimal R)	$n_2/n_0$	1	1	1
	$U_2/U_0$	0.45	0.73	0.80
	$\max C_{p2}/C_{p0}$	0.48	0.69	0.83
	$(C_{T2} + C_{T1})/C_{T0}$	1.59	1.62	1.64
	$\max C_{p2}/C_{p0}$	0.48	0.69	0.83
R-R (optimal R and R)	$n_2/n_0$	0.66	0.88	0.95
	$U_2/U_0$	0.33	0.55	0.68
	$\max C_{p2}/C_{p0}$	0.11	0.39	0.51
	$(C_{T2} + C_{T1})/C_{T0}$	1.32	1.65	1.74
	$\max C_{p2}/C_{p0}$	0.11	0.39	0.51

Table 2 also shows estimations of the axial velocity component  $U_2$  of the incident flow before the second disk or rotor and a ratio  $(C_{T2} + C_{T1})/C_{T0}$  of the total thrust coefficients of all dual setups to the corresponding values of the single cases.

It is clearly seen from the R-R plot, just like any other case of Fig. 1, that the velocity deficit decreases monotonically and in a smooth manner for all the considered cases without large deviation from the fitting G - curve, shown by the solid line. Nevertheless, the wake deficit behind both active rotors (R-R) decreases, as compared to the single samples (R) in contrast to the former dual systems with the forward passive disk (D-D and D-R) when it grows. Next difference of the R-R case indicates by more concentrations of the measuring point along the fitting curve. Hence, we can conclude that the variations of the rotor positions do not have a significant effect on the wake deficit just like other cases with the forward passive disk (D-D and D-R).

### 3. Possible explanations: total thrust, turbulence or near wake impacts

The comparison between the dual passive disks, both passive disk and following active rotor and the dual active rotors shows a strong difference between the wake behaviors in the systems with the forward passive and active obstacles. The evaluation of both wake curves (D-D and D-R) for the passive forward disk indicates an increase in the wake deficit behind the second obstacle, as compared to the single samples (D). In contrast to this, the wake behind the active system of the dual rotors (R-R) decreases, as compared to the single samples (R).

Possible differences in the total thrust behaviors of the passive or active systems were tested and compared as our first idea for this explanation. The thrusts of the disk and rotor systems were measured in [10-11]. The ratio of the total thrust  $(C_{T2} + C_{T1})$  of these dual D-D, D-R and R-R systems to the single samples of D or R ( $C_{T0}$ ) was calculated by varying the distance  $L_x$  (Table 2). For all cases, the flow velocity ( $U_2$ ) in the wake before the second disk or rotor was also estimated and presented in the same table. From this investigation, we can conclude that the total thrust grows for all cases, as compared to the single samples, and it is not clear why the duplication of the passive or active systems results differently in the wake deficit.

Our next step for the explanation of the difference between D-D or D-R and R-R systems concerns the testing of possible differences in the turbulence characteristics. This was tested and Fig. 3 shows the comparison of the distribution of the RMS-values in the wake behind all the considered disk and rotor systems.

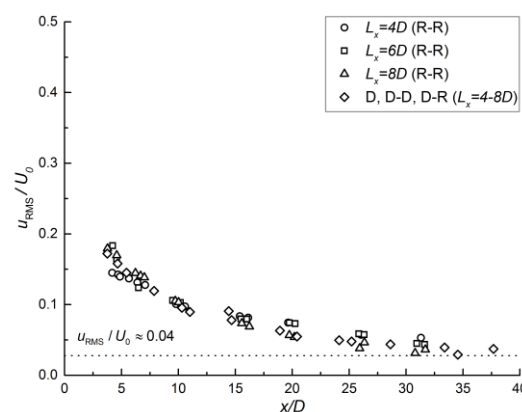


**Figure 3.** A comparison of RMS in the far wakes for both D-D, D-R, and R-R systems.

As seen in the figure the distributions are almost equal. Hence, it can be concluded that it is not the turbulence characteristics that cause the different wake behavior of the different configurations.

One can just guess that a strong influence of the helical tip vortices producing the active systems only to explain these differences. Indeed, the helical vortex system behind rotors plays an important role in a generation of the velocity deficit in the wake. For example, these vortices can reduce the velocity

in the near wake with up to two times as much as in the rotor plane [12-14]. The helical tip vortices are not present when considering the flow about a disk [15]. Thus, the most likely candidate for explaining the different behavior is that the tip vortex in the near wake has an influence on the far wake characteristics in the rotor case.

The properties of the helical tip vortices behind a single rotor and the near wake of a single disk have been studied in many investigations (see e.g. [1, 15-17] and references hereby). In Fig 4 we reproduce profiles of the typical axial velocity distributions in the wakes behind both single rotor and disk to compare them with the ones generating behind the different dual systems on the same distance respectively. The examinations of the new data of the velocity profiles indicate a strong difference in the near wake behavior for the dual passive or active setups as it was found for the velocity deficit in the far wakes (Fig. 1).

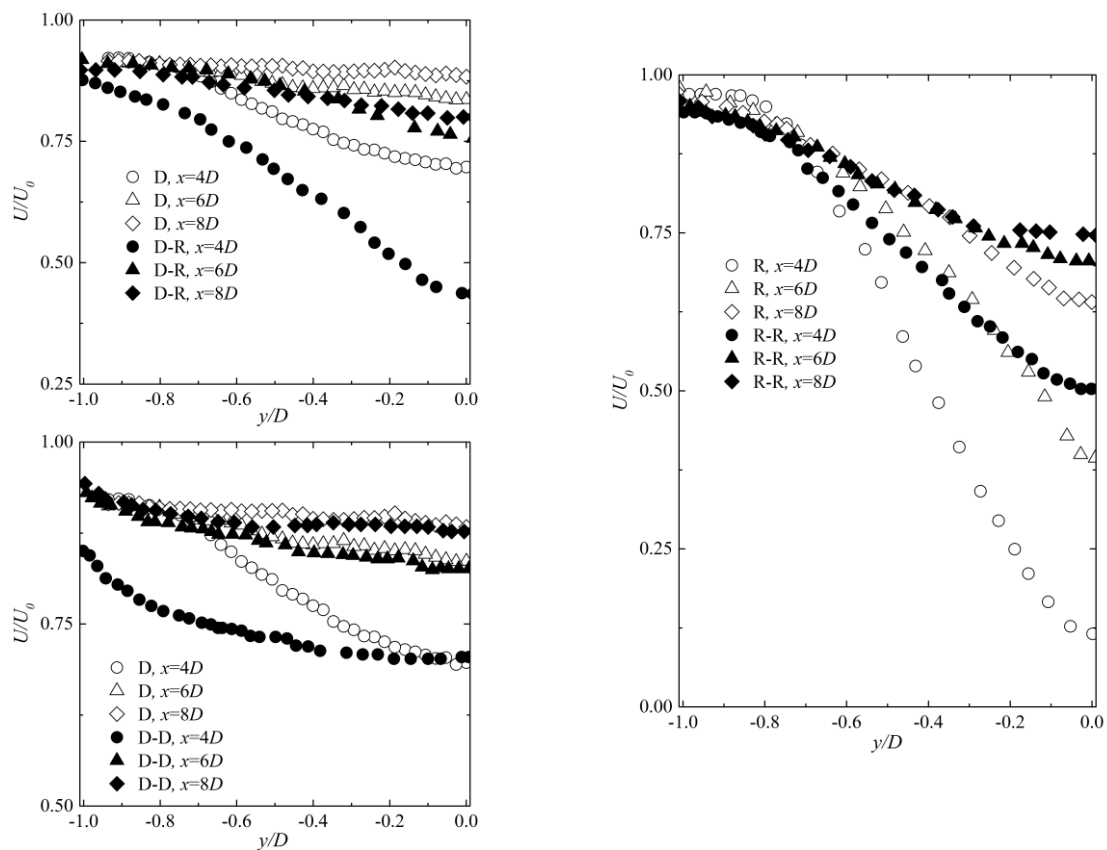


**Figure 4.** A comparison of the axial velocity profiles behind different single and dual testing systems with optimal TSR and  $L_x=8D$ .

Indeed the wake intensity grows for the dual systems when the disks put as the initial passive flow disturbance (for D-D) because the second disk produced an additional resistance in the flow. In contrast to this, the wake intensity behind the dual active rotor system (R-R) becomes smaller than it is behind the single rotor by a reducing of the tip vortex influence in the wake development when the second rotor put in a disturbance. It should also be mentioned that the disturbances coming from the first disk make a very similar “reduction” of the wake profiles behind the second rotor in the dual system D-R to compare with the single rotor (please compare the black symbols on the plots D-R and R-R of Fig. 4).

#### 4. Conclusions

The far wake developments behind the passive and active dual systems (disk-disk; disk-rotor and rotor-rotor) have been studied for different interspatial positions and operating regimes. The measurements show that the velocity deficits in the far wakes for all the considered cases follow a rational dependence with the same rate, but with different wake attenuation coefficients. The resulting velocity deficit of the dual disks strongly depends on the distance between them and the wake intensity grows for the dual disks in comparison with the single one. In contrast to this, the decay of the velocity deficit behind dual rotors is nearly independent of the interspatial distance between them and the wake intensity behind the dual rotor system is smaller than the one behind a single rotor. The differences may be explained by the influence of the rotor tip vortices which are absent in the disk-disk model. Thus, our experiments indicate that a dual disk system cannot satisfactorily replace a system of dual rotors when analyzing wake properties behind wind turbines but the first disk in the disk-rotor system may be used as a method of the tip vortex control in the rotor wake.

#### 5. Acknowledgments

The research was supported by the Russian Science Foundation (Project № 14-19-00487).

#### References

- [1] Okulov VL, Naumov IV, Mikkelsen RF, Kabardin IK, Sørensen JN. A regular Strouhal number for large-scale instability in the far wake of a rotor. *J. Fluid Mech.* 2014; 747: 369-380.
- [2] Okulov VL, Naumov IV, Mikkelsen RF, Sørensen JN. Wake effect on a uniform flow behind wind-turbine model. *Journal of Physics: Conference Series* 2015; 625: 012011.
- [3] Okulov VL, Mikkelsen RF, Naumov IV, Litvinov IV, Gesheva E, Sørensen JN. Comparison of the far wake behind dual rotor and dual disk configurations. *Journal of Physics: Conference Series* 2016; 753: 032060.
- [4] Naumov IV, Kabardin IK, Mikkelsen RF, Okulov VL, Sørensen JN. Rotor performance and wake conditions in non-uniform flow behind an obstacle. *Journal of Physics: Conference Series* 2016; 753: 032051.
- [5] Calaf M, Meneveau C and Meyers J Large eddy simulation study of fully developed wind-turbine array boundary layers. *Phys. Fluids* 2010; 22: 015110
- [6] Porte-Agel F, Wu YT, Chen CH. A numerical study of the effects of wind direction on turbine wakes and power losses in a large wind farm. *Energies*. 2013; 6(10): 5297–5313.
- [7] Nygaard N.G. Wakes in very large wind farms and the effect of neighbouring wind farms. *Journal of Physics: Conference Series* 2014; 524: 012162.
- [8] Naumov IV, Litvinov IV, Mikkelsen RF, Okulov VL. Investigation of a wake decay behind a circular disk in a hydro channel at high Reynolds numbers. *Thermophysics and Aeromechanics* 2015; 22(6): 657-665.
- [9] Naumov IV, Mikkelsen RF, Okulov VL. Estimation of Wake Propagation behind the Rotors of Wind-Powered Generators. *Thermal Engineering* 2016; 63(3): 208–213.
- [10] Okulov VL, Mikkelsen RF, Sørensen JN, Naumov IV, Tsoy MA. Power Properties of Two Interacting Wind Turbine Rotors. *Journal of Energy Resources Technology* 2017; 139(5): 051210.
- [11] Naumov I.V., Litvinov I.V., Mikkelsen R.F., Okulov V.L. Experimental investigation of wake evolution behind a couple of flat disks in the hydro channel. *Thermophysics and Aeromechanics* 2016; 23(5): 657–666.
- [12] Okulov V.L. Limit cases for rotor theories with Betz optimization. *Journal of Physics: Conference Series* 2014; 524: 01212.
- [13] Kuik GAM van, Sørensen JN, Okulov VL. The rotor theories by Professor Joukowski: Momentum Theories. *Prog Aerospace Sci* 2015; 73: 1-18. DOI: 10.1016/j.paerosci.2014.10.
- [14] Okulov VL, Sørensen JN, Wood DH. The rotor theories by Professor Joukowski: Vortex Theories. *Prog Aerospace Sci* 2015; 73: 19-46. DOI: 10.1016/j.paerosci.2014.10.002.
- [15] Naumov IV, Rahmanov VV, Okulov VL, Velte CM, Mayer KE, Mikkelsen RF. Flow diagnostics downstream of a tribladed rotor model. *Thermophysics and Aeromechanics* 2012; 19(2): 171-181.
- [16] Naumov IV, Mikkelsen RF, Okulov VL, Sørensen JN. PIV and LDA measurements of the wake behind a wind turbine model. *Journal of Physics: Conference Series* 2014; 524 (1): 012168
- [17] Bobinski T., Goujon-Durand S., Wesfreid J.E. Instabilities in the wake of a circular disk. *Physical Review E* 2014; 89 (5): 053021